



# Performance and mechanism of bentonite in suppressing methane explosions in a pipeline network

Wang Fengxiao · Jia Jinzhang · Tian Xiuyuan

Received: 19 June 2022 / Accepted: 5 January 2023  
© The Author(s) 2023

**Abstract** Methane explosions threaten the safety of industrial security in modern society. To suppress such explosions, experiments were made through using different masses of bentonite powder driven by CO<sub>2</sub> within a pipe network set up in an independent way. The three factors, including the peak overpressure of an explosion, the index of the explosion power, and the time length within which the first wave of flames reached the pipe network's outlet, were measured to evaluate the performance. Moreover, an analysis on the mechanism of suppressing explosions was also conducted. According to the results, a gradual increase of the powder mass from 20 to 50 g could promote the effect of explosion suppression, but a further increase from 50 g to 60 g only led to a slight improvement of the performance. Thus, it was concluded that the use of 50 g of bentonite powder worked best for the suppression of methane explosions when environmental conservation, energy saving as well as practicality were all taken into consideration. What was found in this study is supposed

to shed theoretical light on how to transport methane safely with disaster risks reduced effectively.

## Article highlights

- (1) Explosion suppression performance of bentonite powder was studied in pipe network.
- (2) The inhibitor parameters with the best performance obtained are more universal.
- (3) The mechanism of explosion suppression was discussed based on molecular dynamics theory.

**Keywords** Methane explosion · Experimental pipe network · Bentonite powder · Explosion suppression performance · Explosion suppression mechanism

## 1 Introduction

Methane is a kind of fuel as well as an important raw material for wide industrial use and manufacturing. However, due to its characteristics of flammability and explosiveness, explosions might occur when methane is transported or utilized (Khan et al. 2017; Qin et al. 2018), which result in not merely enormous economic losses but also irreparable personnel damage (Jia et al. 2022a; Ajrash et al. 2017). For this reason, it is urgent and significant to figure out measures that can effectively suppress methane explosions.

---

Wang Fengxiao and Jia Jinzhang contributed equally to this work.

---

W. Fengxiao · J. Jinzhang (✉) · T. Xiuyuan  
College of Safety Science and Engineering, Liaoning Technical University, Fuxin 123000, Liaoning, China  
e-mail: jiajinzhang@lntu.edu.cn

W. Fengxiao · J. Jinzhang · T. Xiuyuan  
Institute of Safety Science and Engineering, Liaoning Technical University, Fuxin 123000, Liaoning, China

Previous research has suggested using water mists, inert gases, porous media substances, and solid powders to suppress potential methane explosions (Kundu et al. 2016; Jia et al. 2022b, c; Zhou et al. 2021). In the case of employing water mists, its mechanism lies in two aspects, that is, cooling the endothermic process and diluting methane. In a high-temperature environment where evaporation happens continuously, fine water mists can effectively cool down and dilute flammable methane. Besides, the possibilities of methane explosions can also be reduced effectively through suppressing flame structures to be formed (Chen et al. 2021; Wei et al. 2022; Deng et al. 2022). It has been confirmed that inert gases have the effect of diluting flammable gases, delaying the explosion reactions and mass-transfer processes of these gases, and decreasing flame waves' degree of heat transfer. Additionally, inert gases can also lead to the continuous decline of the unburned gas's shock-wave compression, put off the transfer of heat mass from the burned zone to the unburned zone, prevent flame waves from interacting with shock waves, and eventually restrain the extensive formation of flame waves (Zhang et al. 2022, 2021; Zhao et al. 2022). Porous media substances are complicatedly pore-structured, which makes free radicals more likely to collide within pore walls than to engage in explosion reactions, thus mitigating shock waves and reducing flame waves (Yuan et al. 2021; Wang et al. 2020).

Solid powders have the advantages of being pollution-free and easy for storage or transportation, so they have been widely researched as materials to inhibit methane explosions (Li et al. 2022). Powder explosion suppression technology uses a solid powder with fire prevention and extinguishing capabilities and uses its physical or chemical properties to inhibit the spread of a gas explosion flame, reduce the explosion range and reduce the explosion loss (Li et al. 2023; Dong et al. 2022). When a solid powder is utilized as an inhibitor in a flammable gas explosion, its absorption of a huge quantity of heat in the pyrolysis process will result in a dramatic drop in the temperature of the explosion reaction zone and subsequently stop further chain reactions of the explosion. Meanwhile, substances generated from the powder's being pyrolysed will function as free-radical catchers, thereby inhibiting the explosion reaction (Yan et al. 2022; Shi et al. 2022; Zhang et al. 2015). Wang et al. (2017a) conducted gas explosion suppression experiments with

different powders. Their results indicated that the explosion suppression performance of ultrafine ABC powder was better than those of ultrafine silica powder and magnesium hydroxide powder. The small size and surface effect of the ultrafine powder enhanced the chemical activity of the explosion-suppression powder, and the ultrafine powder enhanced its heat absorption capacity during gas explosion. Molecules, atoms, free radicals, etc., from the gas explosion reaction were more easily adsorbed by the inhibitor, the concentrations of free radicals decreased, and the gas explosion was effectively suppressed. Yu et al. (2014) modified waste red mud from the aluminium industry to obtain ultrafine modified red mud powder explosion suppression materials. Through experimental comparisons, it was found that the peak explosion pressure of the modified red mud was reduced by 30% when it was used as an explosion suppressor. Wang et al. (2017b, c) prepared a bicarbonate/red mud composite powder with a core-shell structure by using modified red mud with bicarbonate powder. Their results showed that the explosion suppression performance of the modified sodium bicarbonate/red mud explosion suppression powder was better than that of a single explosion suppression powder. Sun et al. (2019) mixed aluminium hydroxide, ammonium polyphosphate and porous kaolin to obtain a compound powder and tested its explosion suppression performance. The results demonstrated that, compared with a single-component powder, the explosion suppression performance of the modified or composite powder was more prominent.

As a common fuel, methane brings convenience to the national economy and to peoples' lives. However, with increases in daily transportation distances, explosion accidents caused by methane leaks pose serious threats the lives, health and safety of people. There have been few studies focused on suppressing methane explosions in pipeline networks, and the related research is still in its infancy, so the generality and practicability of conclusions obtained from existing studies on suppressing methane explosions in confined spaces are very limited. Therefore, research on effective methods for suppressing methane explosions in pipeline networks is important in improving the safety of methane transport and use. By comprehensively analysing the characteristics of existing powder detonation inhibitors, we found that the molecules in the high-efficiency detonators have large

specific surface areas, layered pore structures and good thermal desorption characteristics, all of which play a role in inhibition of the detonation process (Kang et al. 2016). As a natural metal-based powder, bentonite also has the above characteristics. However, little research has been reported on the use of bentonite for methane explosion suppression.

For the purpose of guaranteeing the security of transporting methane within the existing pipe network, it is of significance to promote the safety level of methane delivery under current conditions with effective collaborative approaches to inhibiting methane explosions. Through experimenting with the utilization of CO<sub>2</sub>-driven bentonite powder to inhibit methane explosions in a pipe network, the study probed into the performance as well as the underlying mechanism of this practice, and what was found is expected to be theoretically referable for personnel and sectors that are responsible for safe transportation and use of methane.

## 2 Experimental setups

### 2.1 Experimental test system

As shown in Fig. 1, the size of the experimental pipe network was 8100 mm × 5500 mm. The experimental system is made up of four components: a pipe network, a system that generates inert gas, a system that gathers real-time data dynamically, and an ignition system. Apart from the core equipment to acquire real-time dynamic data at high speeds (model CR6300), a photo-sensitive flame sensing devices (Model CKG100) and high-accuracy pressure sensing devices (Model CYG1721) were also included in the system for real-time dynamic data collection (Model TST6300). The equipment for acquiring real-time dynamic data had an accuracy of 0.2% FS (on a full scale); both the flame sensing devices and the pressure sensing devices had a response time of 1 ms. As for the ignition system,

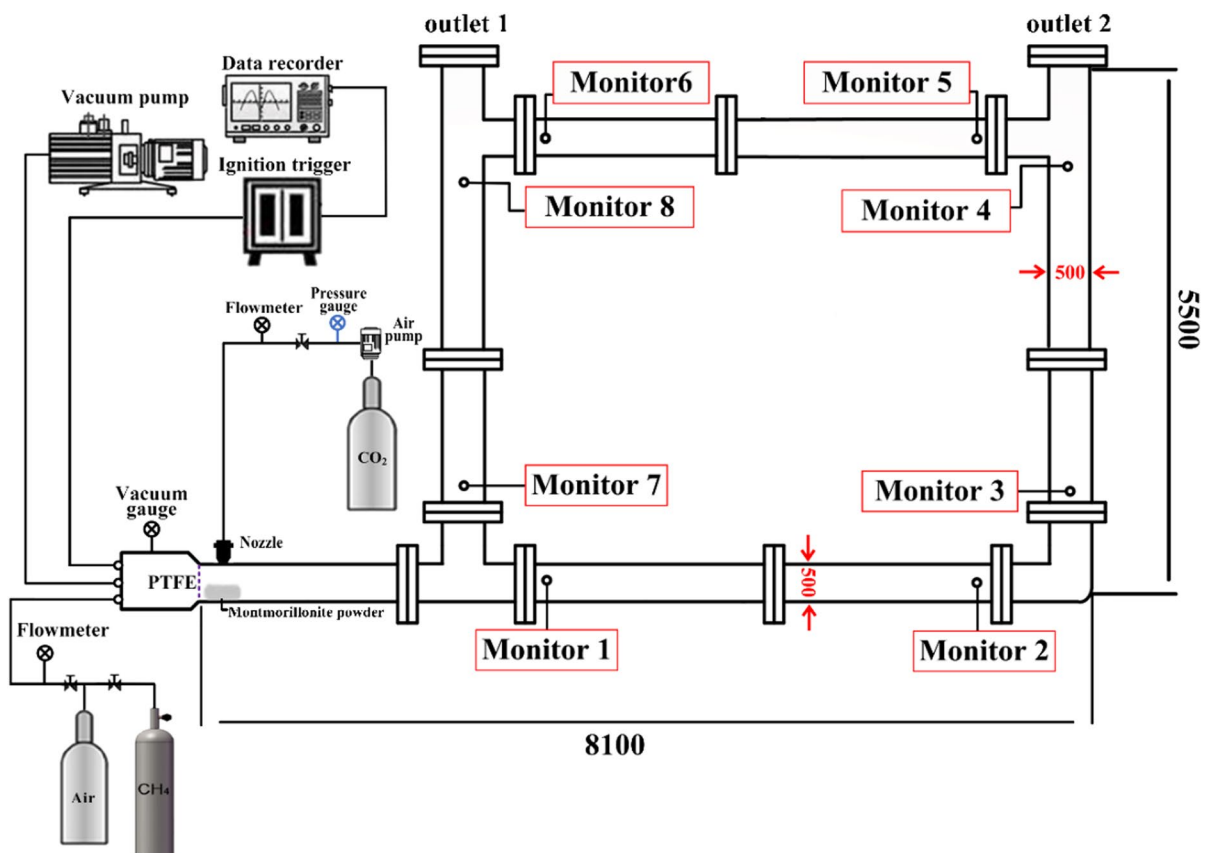


Fig. 1 Experimental system

its main components consisted of a DX-GDH high energy igniter, power cables, cables resistant to high voltages and temperatures, high energy spark plugs at the explosion chamber's front end, and external triggering units to which the ignition control box was linked via a wire. The ignition voltage in the explosion chamber reached approximately 2200 V and it could store 30 J energy at a time.

## 2.2 Experimental procedures

Bentonite powders manufactured by Aladdin Biochemical Technology Corporation in Shanghai were utilized as the experimental samples for methane explosion suppression, whose particle sizes ranged from 28  $\mu\text{m}$  to 46  $\mu\text{m}$  and whose masses varied from 20 g, 30 g, 40 g, 50 g to 60 g. The suspension of bentonite powder particles in the pipe network was driven by 20% volume fraction of  $\text{CO}_2$ , and the pressure for injecting methane was 0.2 MPa (Jia et al. 2022b; Zhang et al. 2022; Wang et al. 2019).

The pipe network was cut off from the explosion chamber using a polytetrafluoroethylene film. As shown in Fig. 1, altogether 8 pressure sensing devices were installed separately at different points for measurement, and 2 flame sensing devices were installed separately at two different outlets in the pipe network to measure the times of flame waves reaching the outlets when the explosion broke out. After pumping the air out of the explosion chamber, methane with 9.5% volume fraction of air was injected into the pipe network. Then, as seen in Fig. 1, bentonite powders were sprinkled on the inner surface of the pipe, following which was jetting air for 15 s (Niu et al. 2019). The next step was to ignite the gas. The external triggering device was switched on; in the meanwhile, the system for acquiring real-time dynamic data began working simultaneously with the igniter. Immediately after switching on the signal light, ignition was performed by way of pressing the start button on the triggering device.

To effectively reduce the errors in measurements of the experimental data, each group of experiments was repeated three times, and the experimental result was taken as the arithmetic mean of the three experiments.

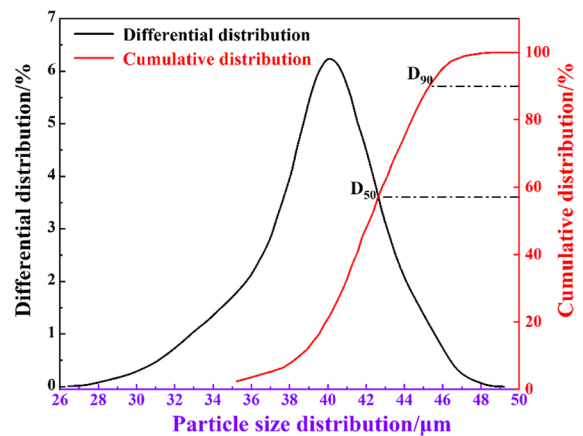


**Fig. 2** Particle size distribution of the powder samples

## 2.3 Powder particle size distribution

Different sizes of sieves were utilized to screen out the sampled bentonite powders of varied sizes. Then, a laser particle-size analyzer (Model Winner 2018) was employed to test how the sampled bentonite powders were distributed in size within the range of the four given particle sizes. The test data is presented in Fig. 2.

According to the data presented above, the sampled bentonite powders intended for the experiment were largely consistent in size, with over 90% of them in conformity to what was required for the bentonite powders in the experiment. Hence, they could satisfy the conditions designed for the explosion.

## 3 Results and discussion

### 3.1 Suppression performance for explosion overpressure peak value

The time-history curves of explosion overpressure at each monitoring point under the action of carbon dioxide driving different masses of bentonite powder are shown in Figs. 3, 4, 5, 6, 7, 8, 9 and 10.

Figure 3 shows the explosion over-pressure experienced many times of fluctuation when no measure was taken to inhibit the explosion, which

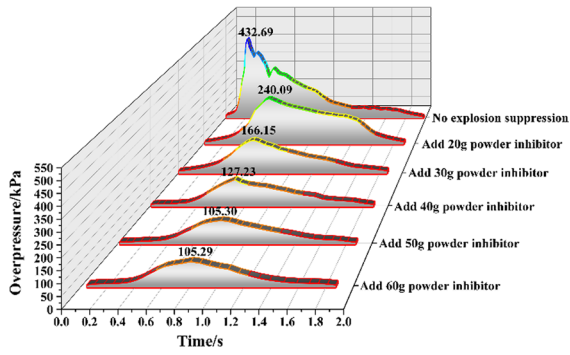


**Fig. 3** Time history change of overpressure at monitoring point 1

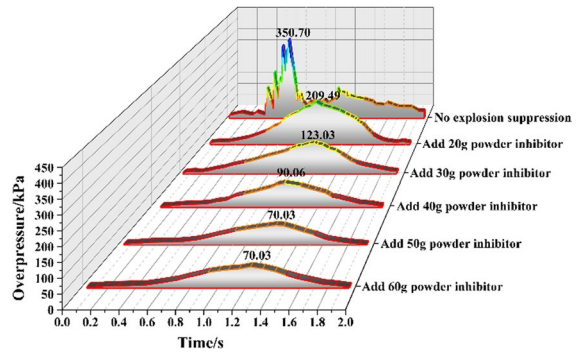


**Fig. 6** Time history change of overpressure at monitoring point 4

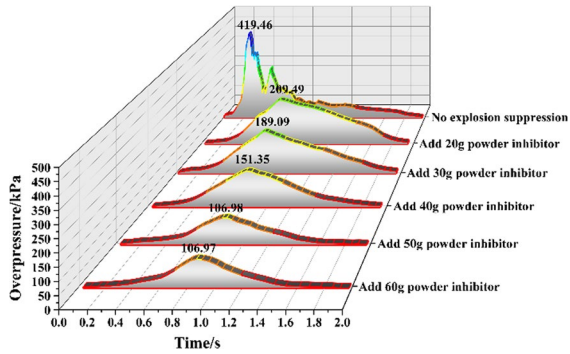


**Fig. 4** Time history change of overpressure at monitoring point 2

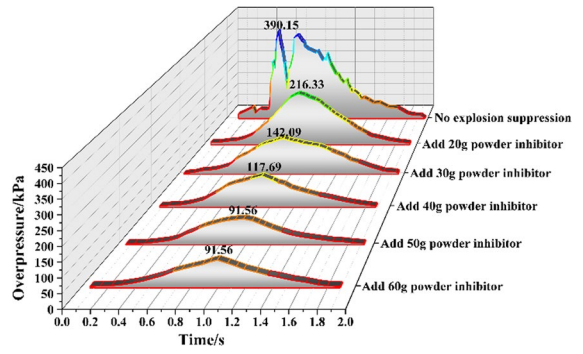


**Fig. 7** Time history change of overpressure at monitoring point 5

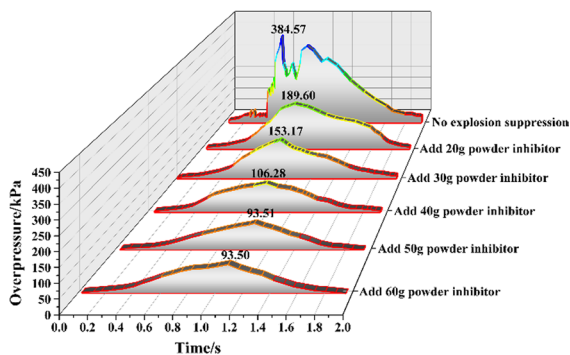


**Fig. 5** Time history change of overpressure at monitoring point 3

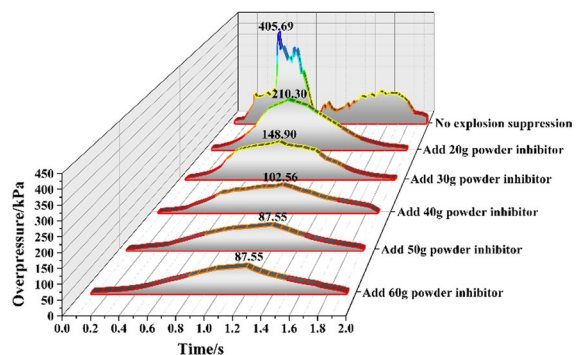


**Fig. 8** Time history change of overpressure at monitoring point 6

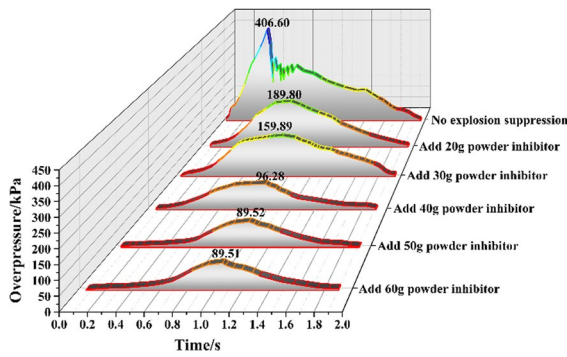


**Fig. 9** Time history change of overpressure at monitoring point 7

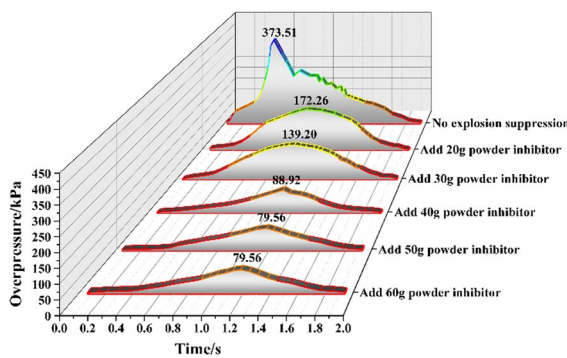


**Fig. 10** Time history change of overpressure at monitoring point 8

implies many times of super-positions and hedging occurred to the explosion shock wave during the entire spreading process. This was attributed to the special structure of the pipe network, where the explosion shock wave was propagated in a disordered and complicated manner. In this case, the explosion over-pressure reached many times of high point, and the highest one was 432.69 kPa. However, a sequence of suppression treatments resulted in the weakening and ultimate disappearance of the disordered and complicated shock wave, and led to the explosion over-pressure only reaching one single peak.

In general, the overpressure evolution processes for the other monitoring points were similar to that for monitoring point 1. As shown in Figs. 4, 5, 6, 7, 8, 9 and 10, when the mass of bentonite powder was increased from 20 g gradually to 50 g, all monitoring points saw their highest value of the

explosion over-pressure declining remarkably, but when the mass of bentonite powder was increased to the level of 60 g, the outcome was different: half of the 8 monitoring points (1, 2, 3, 7) witnessed a slight decline in the peak over-pressure while the other half monitoring points (4, 5, 6, 8) remained unchanged. This result disclosed that, within the pipe network, all the 8 monitoring points would see their peak over-pressure value go downward when the mass of bentonite powder was increased gradually within the range from 20 to 50 g, and that the monitoring points near the explosion source would experience a slight decline in the peak over-pressure value when the mass of bentonite powder was increase from 50 to 60 g while those distant monitoring points away from the explosion source would see no change in the peak over-pressure value. To be put in another way, 60 g or above of bentonite powder exerted certain but insignificant effect on the suppression of methane explosion in the monitoring points near the explosion source, and no effect at all in those distant from the explosion center.

### 3.2 Suppression performance for the explosion power index

The average rate of increase in the explosion over-pressure is defined as:

$$v = \frac{P_{\max} - P_0}{\Delta t} \quad (1)$$

where  $P_{\max}$  represents the explosion over-pressure's highest value (kPa),  $P_0$  stands for the explosion over-pressure's initial value (kPa), and  $\Delta t$  represents the time length during which the explosion over-pressure rose from the initial value to the highest value.

The destructive force of a methane explosion is primarily measured by the explosive power index, which is represented as follows (Yang et al. 2018):

$$K = P_{\max} v \quad (2)$$

where  $K$  is the power index ( $10^{11} \text{ Pa}^2/\text{s}$ ),  $P_{\max}$  is the peak value of the explosion overpressure (kPa), and  $v$  is the average rate of increase in the explosion over-pressure (kPa/s).

Equation (1) measured at what rates on average the explosion over-pressures changed at all monitoring points when different masses of

**Table 1** Overpressure peak values and overpressure rise rates at each monitoring point under all operating conditions

Mass of powder (g)	$M_1$		$M_2$		$M_3$		$M_4$		$M_5$		$M_6$		$M_7$		$M_8$	
	$P_{max}$	$\nu$	$P_{max}$	$\nu$	$P_{max}$	$\nu$	$P_{max}$	$\nu$	$P_{max}$	$\nu$	$P_{max}$	$\nu$	$P_{max}$	$\nu$	$P_{max}$	$\nu$
0	450.28	2145.2	393.19	1554.1	370.53	630.15	334.19	537.29	367.58	519.92	396.95	763.36	406.23	933.86	399.43	746.99
20	231.67	367.73	192.08	255.76	177.16	201.32	166.27	165.45	188.95	214.72	195.19	250.24	200.16	236.87	196.37	213.33
30	159.28	248.09	145.63	175.03	140.57	147.19	108.39	102.93	138.68	148.79	146.93	166.96	150.78	159.39	149.24	146.73
40	109.87	161.58	83.21	90.58	79.87	79.95	63.72	57.93	83.27	83.19	88.09	88.45	93.96	86.97	89.38	80.24
50	87.21	101.39	73.67	70.49	69.78	66.36	50.83	44.33	70.66	62.48	75.56	66.28	82.19	70.54	78.12	65.23
60	87.19	101.13	73.65	70.42	69.77	66.35	50.83	44.33	70.66	62.48	75.56	66.28	82.17	70.53	78.12	65.23

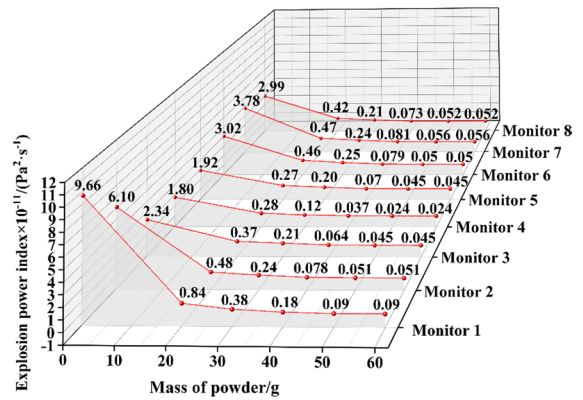


**Fig. 11** Explosion power index of each monitoring point under different conditions

CO<sub>2</sub>-driven bentonite powder were utilized to suppress the experimental methane explosion (as seen in Table 1). Then, all monitoring points' explosion power indexes were obtained by combining Eq. (2) with the data about the average changing rates of the explosion over-pressures at all monitoring points, as shown in Fig. 11.

Figure 11 presents how all the monitoring points explosion power indexes changed when different masses of CO<sub>2</sub>-driven bentonite powder were used to inhibit the explosion. As shown in Fig. 11, the changing tendencies of all monitoring points' explosion powder indexes are in consistency with the changing tendencies of their over-pressure peak values when different masses of CO<sub>2</sub>-driven bentonite powder were used, which indicates some kind of correlation between the two group of values. With the mass of CO<sub>2</sub>-driven bentonite powder increased from 20 to 50 g, all monitoring points' explosion power indexes were dropping evidently. Afterwards, with the mass of bentonite powder increased to 60 g continuously, all monitoring points' explosive power indexes kept almost the same.

When the mass of bentonite powder was increased continuously above the critical value of 50 g, all the 8 monitoring points varied slightly in the peak explosion over-pressure, but their explosion power indexes showed consistent changing tendencies. Under the conditions of applying 60 g bentonite powder to the pipe network, certain monitoring points did see a slight decline in the peak explosion over-pressure, but their explosion power indexes were almost the same

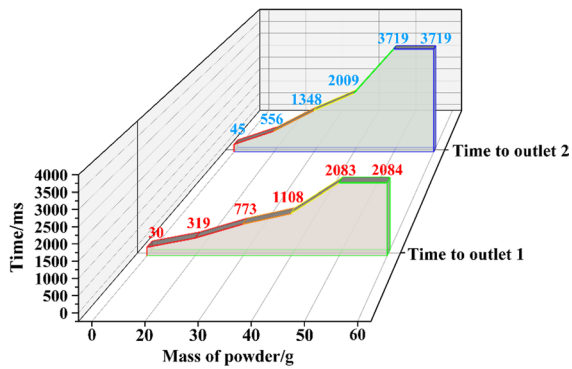


**Fig. 12** Time for the flame wave to reach the two outlets under different working conditions

as those when 50 g of bentonite powder was applied, which implied that the effect of utilizing 60 g of bentonite powder to inhibit methane explosion shock waves showed no difference from that of using 50 g of bentonite powder. This finding supports the conclusion that the optimal amount of bentonite powder applied to the pipe network for the inhibition of methane explosion over-pressures was 50 g.

### 3.3 Suppression performance for explosion flame wave fronts

Figure 12 presents the changing tendencies of time lengths during which explosion flame waves rushed at two different pipe network outlets under the conditions that different masses of CO<sub>2</sub>-driven bentonite powder were utilized to suppress the explosion. As disclosed in Fig. 12, it took much less time for the flame waves to arrive at Outlet 1, which was due to the shorter distance of Outlet 1 from the explosion source when compared with Outlet 2. With the mass of bentonite powder increased gradually from 20 to 30 g to 40 g and to 50 g, the flame waves were inhibited from further spreading, and the time lengths that flame waves required to arrive at the two pipe network outlets were growing longer. Under the conditions of applying 50 g of bentonite powder, its performance of suppressing the flame waves from being propagated reached the peak. However, when the mass of bentonite powder was continuously increased to 60 g, the time that the flame waves required to get to Outlet 1 was only prolonged for 1 ms, and the time that the flame waves required to get to Outlet 2 was

almost the same as that in the case of using 50 g of bentonite powder. On the whole, the way of increasing the amount of bentonite powder from 50 to 60 g exerted weak effect on the further inhibition of flame waves from spreading. Thereby, taking practicality into consideration, the application of 50 g of bentonite powder to the inhibition of flame waves of a methane explosion could achieve the best performance.

### 3.4 Discussion

Previous research on the utilization of a specific substance to inhibit methane explosions is based largely on experiments made in horizontal straight pipes or spherical containers with fixed volumes, which is evidently limited (Jiang et al. 2021; Shang et al. 2019). For this reason, we experimented with using varied masses of CO<sub>2</sub>-driven bentonite powder to suppress methane explosions in the environment of a pipe network. When no measure is taken to inhibit methane explosions, shock waves as well as flame waves spread in a disordered and nonlinear manner. Furthermore, the explosion power index as well as the over-pressure peak does not decline regularly in a linear manner with the distance increased from the explosion center. But the bentonite powder achieved the best effect in suppressing the methane explosion in the unique structure of the pipe network when examined by measuring the time spent by the flame waves arriving at two separate outlets of the pipe network. With the powder mass added from 20 g gradually to 50 g, the flame wave spreading to the more distant outlet witnessed a large time increment gradient. Such features were not observed when explosion suppression experiments were performed in horizontal straight pipes or spherical containers. Hence, it could be said that the unique structure of a pipe network was conducive to the inhibition of a methane explosion particularly when the optimal conditions were created for that. Besides, all the eight monitoring points saw their highest explosion over-pressures as well as explosion power indexes change linearly in the pipe network, which was similar to but was not totally the same as the changing pattern in the environment of a straight horizontal pipe. Though this finding only justifies the need to investigate into the inhibition of methane explosions in a pipe network, it is still a universally applicable conclusion that 50 g of CO<sub>2</sub>-driven bentonite powder had the best effect



on suppressing methane explosions within the unique structure of pipe networks.

In brief, through examining the three parameters of highest explosion over-pressures, explosion power indexes as well as the time lengths consumed by flame waves to arrive at the pipe network’s two separate outlets, it is concluded that a mass of CO<sub>2</sub>-driven bentonite powder, ideally not exceeding 50 g, has significant effect on methane explosion inhibition through stopping flame waves as well as shock waves from further propagating. A mass of bentonite powder that exceeds 50 g, however, cannot enhance this effect in the actual situation of pipe-networked explosion inhibition but merely leads to accumulated dust, which not only increases environmental burden but also gives rise to waste of energy and resources. Furthermore, excessive masses of the suppressant also have the potential to interfere with the real suppression outcome (Bu et al. 2020; Dai et al. 2022). Out of these considerations based on the experimental observation and results, 50 g is suggested as the optimal mass when CO<sub>2</sub>-driven bentonite powder is utilized for the inhibition of methane explosions in the environment of pipe networks, and the highest suppressive performance can be fulfilled in this case.

#### 4 Discussion of the explosion suppression mechanism

Bentonite powder is prone to thermal decomposition because of its pyrolytic properties, which determines

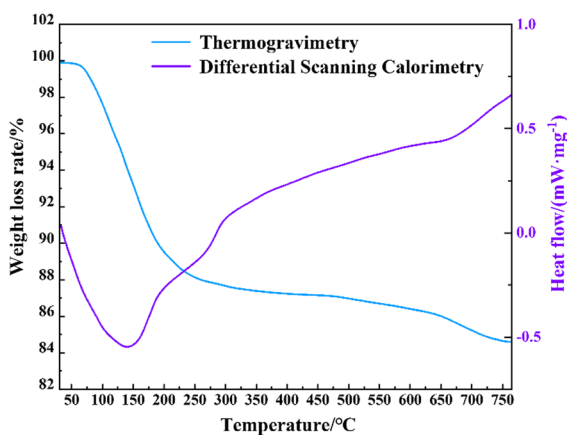


Fig. 13 TG-DSC curve of the bentonite powder

its high performance in absorbing heat. Such material characteristics indicate that bentonite powder can chemically restrain the spread of flame waves away from the central point by inhibiting the chain reaction of a methane explosion. Additionally, as carbon dioxide has chemical as well as physical effects of suppressing gas explosions, a methane explosion can be inhibited both chemically and physically by utilizing CO<sub>2</sub>-driven bentonite powder (Uddin 2008; Babushok et al. 2017).

With regard to bentonite powder’s physical effect of inhibiting explosions, it is presented in Fig. 13 through the curves of thermogravimetry–differential scanning calibration (TG-DSC). Structural water gets lost when a water molecule is formed by releasing two hydroxyl groups (Guo et al. 2005). Moreover, the bentonite powder is able to absorb 279.36 J/g of energy when pyrolyzed. These results confirm that bentonite powder’s pyrolytic properties are outstanding. In the experimental methane explosion, when the bentonite powder was decomposed with heat, water vapor was released. This led to the dilution of oxygen as well as the absorption of much heat, which thereby suppressed the reaction process. Since in the explosion reaction, the loss of heat surpassed the release of heat, the environmental temperature dropped below the ignition point of methane. Therefore, the methane explosion was physically suppressed to some degree. Additionally, CO<sub>2</sub> is an inert gas able to lower the fuel–air ratio. Through decreasing reactants’ concentration in the explosive reaction, CO<sub>2</sub> can hinder heat from transferring to the flammable gas. Particularly,

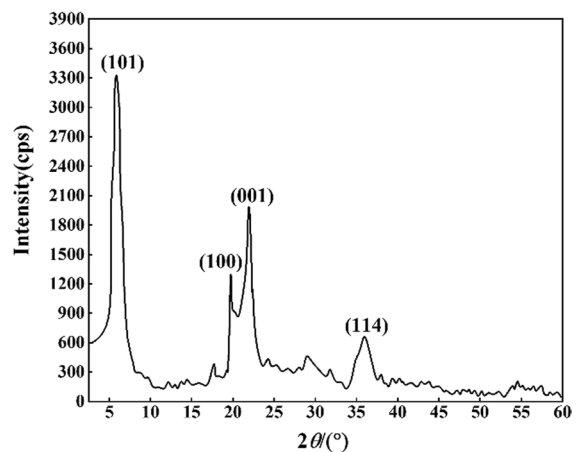
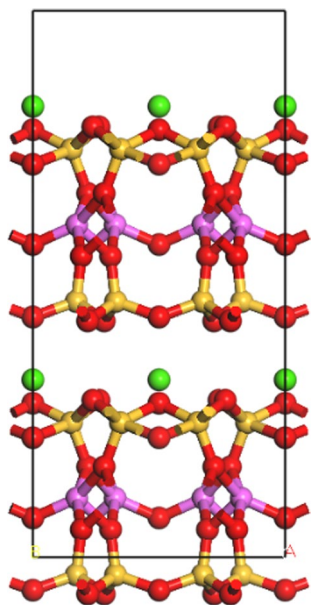


Fig. 14 Molecular XRD analysis result



**Fig. 15** Bentonite single-cell molecular model

it produces an environment where oxygen molecules are less likely to come into contact with the flammable gas, thus reducing the effective surface of their contact and ultimately inhibiting the explosion physically (Okulik and Jubert 2003).

To understand chemical suppression, the XRD results for bentonite powder are shown in Fig. 14. Based on these results, the most active (101) plane of the bentonite crystals was used to analyse its molecular characteristics.

In this paper, crystal structure parameters were predicted in detail and compared with the results from experiments, which verified the rationality of the calculated parameters.

Figure 15 shows the single unit cell model established by optimization of the bentonite (101) crystalline plane. In the figure below, the yellow balls represent silicon atoms, the red balls represent oxygen atoms, the pink balls represent aluminium atoms, and the green balls represent calcium atoms.

The combustion and explosion flames for hydrocarbons such as methane contain positive and negative ions, and most of them are positive ions. The flame has a positive potential overall, and large numbers of active radicals, such as  $\cdot\text{O}$  and  $\cdot\text{H}$ , are generated in the explosion flame. It has been confirmed that electric charge affects the probability of collisions

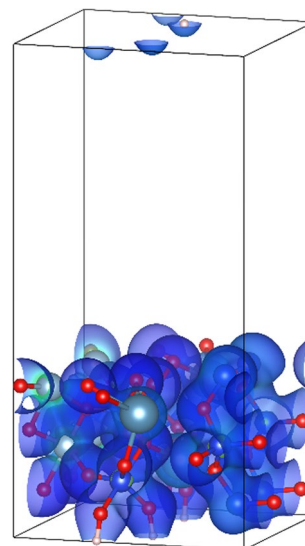


**Fig. 16** Bentonite single-cell molecular model

between reactive radicals in a flame (Wang et al. 2022a). Therefore, studying the electrostatic properties of explosion-suppression powders can reveal the microscopic reactions occurring between these powders and radicals in the flame.

Figure 16 shows an isosurface diagram for the surface electrostatic potential of the bentonite molecular model. The isosurface value was set to 0.025, and the areas where the electrostatic potential is negative are blue.

As illustrated in Fig. 16, the bentonite molecules have negative charges on the surface, and these charges were aggregated by van der Waals forces. This proved that bentonite was easily attacked by electrophiles. Using this phenomenon, it can be understood from a macro perspective that bentonite serves as an inhibitor of reactions between methane and oxygen, the reactants are continuously consumed during the overall reaction process, and the concentrations of the reactants are effectively reduced, which suppresses the explosion.

When bentonite powder is dehydrated thermally, metal ions are released and come into combination with  $\cdot\text{O}$ ,  $\text{H}\cdot$ . Then the generated  $\cdot\text{OH}$  acted as a reactant to participate in the chemical reaction of the methane explosion (Wang et al. 2022b). The chain reaction after suppression is changed to  $\text{O} + \text{CO} + \text{M} \rightarrow \text{CO}_2 + \text{M}$ ,  $\text{O} + \text{HCO} \rightarrow \text{H} + \text{CO}_2$ ,

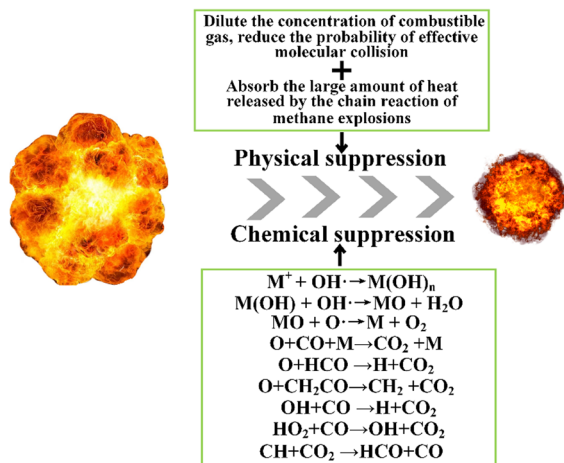
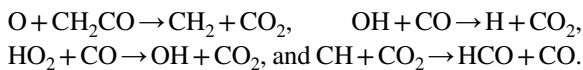


**Fig. 17** Explosion suppression mechanism diagram



A series of reactions described above play a role of combining with free radicals that are released in the chain reaction of the methane explosion. In this way, less free radicals are left to participate in the subsequent explosive reaction, which reduces the speed of the the methane explosive reaction and hence causes chemical inhibition in the end (Li et al. 2019).

In summary, the specific process of carbon dioxide-driven bentonite powder to suppress methane explosion in pipe networks is shown in Fig. 17.

## 5 Conclusions

The main conclusions of this study are summarized as follows:

1. The physical properties of bentonite powder, which is easily decomposed by heat, determine that it has good endothermic properties. The total energy absorbed by bentonite powder during the whole pyrolysis process was 279.36 J/g. Furthermore, the negative charges on the surface of bentonite molecules are easily attacked by electrophiles (such as methane), the reactants are continuously consumed during the whole reaction process, the concentration of reactants is effectively reduced, and the methane explosion is suppressed.

2. The flame waves as well as the shock waves in a methane explosion can be effectively inhibited from propagating in a pipe network by employing CO<sub>2</sub>-driven bentonite powder. This inhibiting effect could be gradually strengthened through increasing the mass of bentonite powder from the initial 20 g to 50 g, but it would decline when the powder mass was continuously increased to 60 g. Hence, with environmental conservation, energy saving and practicality taken into comprehensive consideration, 50 g of bentonite powder was the optimal volume when applied to the inhibition of methane explosions as it achieved the best performance.
3. The unique structure of a pipe network was conducive to the inhibition of a methane explosion particularly when the optimal conditions were created for that. Besides, all the eight monitoring points saw their highest explosion over-pressures as well as explosion power indexes change linearly in the pipe network, which was similar to but was not totally the same as the changing pattern in the environment of a straight horizontal pipe. Though this finding only justifies the need to investigate into the inhibition of methane explosions in a pipe network, it is still a universally applicable conclusion that 50 g of CO<sub>2</sub>-driven bentonite powder had the best effect on suppressing methane explosions within the unique structure of pipe networks.

**Acknowledgements** This work was supported by the National Natural Science Foundation of China (grant number 52174183).

**Author contributions** WF: Performed the experiment, manuscript preparation and writing original manuscript. JJ.: Formal analysis and contributed to the conception of the study. TX: Contributed significantly to the data analysis.

### Declarations

**Conflict of interest** The authors declare that they have no competing interests that could have appeared to influence this paper.

**Open Access** This article is licensed under a Creative Commons Attribution 4.0 International License, which permits use, sharing, adaptation, distribution and reproduction in any medium or format, as long as you give appropriate credit to the original author(s) and the source, provide a link to the Creative

Commons licence, and indicate if changes were made. The images or other third party material in this article are included in the article's Creative Commons licence, unless indicated otherwise in a credit line to the material. If material is not included in the article's Creative Commons licence and your intended use is not permitted by statutory regulation or exceeds the permitted use, you will need to obtain permission directly from the copyright holder. To view a copy of this licence, visit <http://creativecommons.org/licenses/by/4.0/>.

## References

- Ajrash M, Zanganeh J, Moghtaderi B (2017) Deflagration of premixed methane-air in a large-scale detonation tube. *Process Saf Environ Prot* 109:374–386
- Babushok V, Linteris G, Hoorelbeke P et al (2017) Flame inhibition by potassium-containing compounds. *Combust Sci Technol* 189:2039–2055
- Bu Y, Li C, Amyotte P et al (2020) Moderation of Al dust explosions by micro- and nano-sized  $Al_2O_3$  powder. *J Hazard Mater* 381:120968
- Chen B, Feng X, Zhang H et al (2021) Experimental study on suppression of methane-coal dust compound explosion by ultra-fine water mist. *Fire Sci Technol* 40(07):1046–1051
- Dai H, Liang G, Yin H et al (2022) Experimental investigation on the inhibition of coal dust explosion by the composite inhibitor of carbamide and zeolite. *Fuel* 308:121981
- Deng T, Norris S, Sharma R (2022) Effects of the water spray system on the air-driving force required in longitudinally ventilated road tunnels. *Tunn Undergr Space Technol* 130:104753
- Dong Z, Liu L, Chu Y et al (2022) Explosion suppression range and the minimum amount for complete suppression on methane-air explosion by heptafluoropropane. *Fuel* 328:125331
- Guo Z, Xing R, Liu S et al (2005) The synthesis and antioxidant activity of the Schiff bases of chitosan and carboxymethyl chitosan. *Bioorg Med Chem Lett* 15(20):4600–4603
- Jia J, Wang F, Li J et al (2022a) Propagation characteristics of the overpressure waves and flame fronts of methane explosions in complex pipeline networks. *Geomat Nat Haz Risk* 13(1):54–74
- Jia J, Wang F, Tian X (2022b) Study on methane explosion suppression in diagonal pipe networks using a fine water mist containing KCl and an inert gas. *ACS Omega* 7(37):32959–32969
- Jia J, Tian X, Wang F (2022c) Study on the effect of  $KHCO_3$  particle size and powder spraying pressure on the methane explosion suppression characteristics of pipe networks. *ACS Omega* 7(37):31974–31982
- Jiang H, Bi M, Zhang T et al (2021) A novel reactive P-containing composite with an ordered porous structure for suppressing nano-Al dust explosions. *Chem Eng J* 416:129156
- Kang X, Gollan R, Jacobs P et al (2016) Suppression of instabilities in a premixed methane-air flame in a narrow channel via hydrogen/carbon monoxide addition. *Combust Flame* 173:266–275
- Khan I, Othman M, Hashim H et al (2017) Biogas as a renewable energy fuel—a review of biogas upgrading, utilisation and storage. *Energy Convers Manage* 150:277–294
- Kundu S, Zanganeh J, Moghtaderi B (2016) A review on understanding explosions from methane-air mixture. *J Loss Prev Process Ind* 40:507–523
- Li M, Xu J, Wang C et al (2019) Thermal and kinetics mechanism of explosion mitigation of methane-air mixture by  $N_2/CO_2$  in a closed compartment. *Fuel* 255:115747
- Li Y, Chen X, Yuan B et al (2022) Synthesis of a novel prolonged action inhibitor with lotus leaf-like appearance and its suppression on methane/hydrogen/air explosion. *Fuel* 329:125401
- Li Y, Zhao Q, Chen X et al (2023) Effect of copper foam on the explosion suppression in hydrogen/air with different equivalence ratios. *Fuel* 333:126324
- Niu Y, Shi B, Jiang B (2019) Experimental study of overpressure evolution laws and flame propagation characteristics after methane explosion in transversal pipe networks. *Appl Therm Eng* 154:18–23
- Okulik N, Jubert AH (2003) Theoretical analysis of the reactive sites of non-steroidal anti-inflammatory drugs. *Internet Electron J Mol Des* 4(01):17–30
- Qin Y, Moore TA, Shen J et al (2018) Resources and geology of coalbed methane in China: a review. *Int Geol Rev* 60(5–6):777–812
- Shang S, Ma X, Yuan B et al (2019) Modification of halloysite nanotubes with supramolecular self-assembly aggregates for reducing smoke release and fire hazard of polypropylene. *Compos Part B Eng* 177:107371
- Shi Z, Zheng L, Zhang J et al (2022) Effect of initial pressure on methane/air deflagrations in the presence of  $NaHCO_3$  particles. *Fuel* 325:124910
- Sun Y, Yuan B, Chen X et al (2019) Suppression of methane/air explosion by kaolinite-based multi-component inhibitor. *Powder Technol* 343:279–286
- Uddin F (2008) Clays, nanoclays, and montmorillonite minerals. *Metall and Mater Trans A* 39(12):2804–2814
- Wang X, Kong L, Xu H et al (2017a) Suppression of methane / air flame propagation in large scale pipelines by clouds of ultrafine powders. *J China Coal Soc* 42(6):1482–1488
- Wang Y, Cheng Y, Yu M et al (2017b) Methane explosion suppression characteristics based on the  $NaHCO_3$ /red-mud composite powders with core-shell structure. *J Hazard Mater* 335:84–91
- Wang Y, Cheng Y, Cao J et al (2017c) Suppression characteristics of  $KHCO_3$ /red-mud composite powders with core-shell structure on methane explosion. *J China Coal Soc* 42(3):653–658
- Wang Y, Ying H, Meng H et al (2019) Investigation of the effect of montmorillonite powders on gas explosion parameters. *Trans Beijing Inst Technol* 39(02):111–117
- Wang L, Liang Y, Hu Y et al (2020) Synergistic suppression effects of flame retardant, porous minerals and nitrogen on premixed methane/air explosion. *J Loss Prev Process Ind* 67:104263
- Wang F, Jia J, Tian X (2022a) Suppression of methane explosion in pipeline network by carbon dioxide-driven calcified montmorillonite powder. *Arab J Chem* 15(10):104126

- Wang F, Jia J, Tian X (2022b) Suppression of methane explosion in a pipe network by carbon dioxide-driven montmorillonite powder with different masses. *Int J Energy Res*. <https://doi.org/10.1002/er.8631>
- Wei S, Yu M, Pei B et al (2022) Length experimental and numerical study on the explosion suppression of hydrogen/dimethyl ether/methane/air mixtures by water mist containing  $\text{NaHCO}_3$ . *Fuel* 328:125235
- Yan L, Wang N, Xu Z (2022) Experimental study on the effectiveness and safety of cement powder on extinguishing metal magnesium fires based on pneumatic conveying technology. *Case Stud Therm Eng* 37:102279
- Yang K, Ji H, Xing Z et al (2018) Characteristics on methane explosion suppression by ultrafine water mist containing potassium oxalate. *CIESC J* 69(12):5359–5369
- Yu M, Kong J, Wang Y et al (2014) Experimental research on gas explosion suppression by modified red mud. *J China Coal Soc* 39(7):1289–1295
- Yuan B, Zhang Y, Yuan Y et al (2021) Study on explosion suppression performance of porous polypropylene. *China Saf Sci J* 31(8):91–96
- Zhang X, Yu S, Kang K (2015) Experimental study on explosion suppression property of phosphorus pentoxide powder. *Coal Technol* 34(12):179–181
- Zhang S, Bi M, Jiang H et al (2021) Suppression effect of inert gases on aluminium dust explosion. *Powder Technol* 59:90–99
- Zhang S, Ma H, Huang X et al (2022) Numerical simulation on natural gas explosion and prevention measures design under water-gas compartment in utility tunnel. *Tunn Undergr Space Technol* 130:104754
- Zhao Q, Li Y, Chen X (2022) Fire extinguishing and explosion suppression characteristics of explosion suppression system with  $\text{N}_2/\text{APP}$  after methane/coal dust explosion. *Energy* 257:124767
- Zhou Y, Li Y, Jiang H et al (2021) Investigations on unconfined large-scale methane explosion with the effects of scale and obstacles. *Process Saf Environ Prot* 155:1–10

**Publisher's Note** Springer Nature remains neutral with regard to jurisdictional claims in published maps and institutional affiliations.